American Mineralogist, Volume 84, pages 1406–1414, 1999

Rietveld refinement of the crystallographic structure of human dental enamel apatites

R.M. WILSON,[1,*] J.C. ELLIOTT,[1] AND S.E.P. DOWKER[2]

[1]Department of Biophysics in Relation to Dentistry, St. Bartholomew's and the Royal London School of Medicine and Dentistry, Queen Mary and Westfield College, Mile End Road, London E1 4NS, U.K.

[2]Comprehensive Dental Care Section, St. Bartholomew's and the Royal London School of Medicine and Dentistry, Queen Mary and Westfield College, Turner Street, London E1 2AD, U.K.

ABSTRACT

Rietveld refinements using 12 sets of X-ray diffraction powder data from milligram samples of human dental enamel provide detailed information about the structure and composition of enamel apatite. The principal difference in atomic parameters between enamel apatite and Holly Springs hydroxylapatite is in O2, which is reflected in a reduction in the P-O2 bond length of 0.085 Å and PO_4 volume by 3.6%. Modeling the hexad axis scattering with a single OH^- ion gives a 0.089 Å shift of the ion further away from the mirror plane at $z = ¼$. The known distributed electron density along the hexad axis in enamel has been confirmed by direct comparison with synthetic hydroxylapatite. Although the CO_3^{2-} ion position could not be determined directly, evidence for partial replacement of PO_4^{3-} by CO_3^{2-} ions came from an 8% diminution of the P site occupancy compared with that in stoichiometric hydroxylapatite. The observed reduction in the P-O2 bond length and PO_4 volume in enamel is also consistent with this substitution. The loss of negative charge caused by CO_3^{2-} replacing PO_4^{3-} ions and loss of OH^- ions is compensated by loss of Ca^{2+} ions from Ca2 sites. The calculated density from the X-ray results is 3.021 g/cm^3, in agreement with deductions from previous chemical analyses.

INTRODUCTION

X-ray powder diffraction and chemical analyses show that mammalian dental enamel apatite is an impure form of hydroxylapatite, $Ca_{10}(PO_4)_6(OH)_2$ (structure described in Elliott 1994). The major difference of enamel apatite from hydroxylapatite is in the presence of about 3 wt% CO_3. Details of the crystallographic structures of carbonate-containing apatites (including minerals) are important because CO_3^{2-} ions increase their reactivity, both in thermal and aqueous systems. For example, enamel from a caries lesion contains less carbonate than normal enamel. However, it is not clear whether this is because the mineral has dissolved and some reprecipitated with less carbonate, or a more soluble, carbonate-rich fraction of the mineral has preferentially dissolved. These possibilities can only be distinguished if subtle structural changes can be characterized.

Enamel apatite crystals are too small for single-crystal structure determination, but unit-cell contents have been deduced from chemical analyses assuming that tetrahedral sites are full (Table 1). The OH^- ion content is deduced from the requirement for charge balance assuming that CO_3^{2-} ions only replace PO_4^{3-} ions (except the last formula in which a small fraction also replaces OH^- ions). Compared to hydroxylapatite, these formulae show a deficiency of ions in Ca^{2+} and OH^- ion sites. The loss of negative charge from the loss of OH^- ions and replacement of PO_4^{3-} by CO_3^{2-} ions is balanced by loss of positive charge from Ca^{2+} sites.

Polarized infrared (IR) spectroscopy of sections of enamel (reviewed in Elliott 1994) shows that the OH^- ions lie parallel to the *c*-axis, with evidence for perturbation of some OH^- by neighboring Cl^- ions. Such studies also show that the CO_3^{2-} ions are oriented with respect to the apatite lattice and are probably in two different environments. The majority of the CO_3^{2-} ions have their planes oblique to the *c*-axis and are thought to occupy the sloping faces of tetrahedral sites. The minority of ions, comprising about 10% of the total, have their planes nearly parallel to the *c*-axis and are thought to occupy sites in the hexad axis channel.

The Rietveld whole pattern fitting method (Young 1993) was applied to neutron and X-ray powder diffraction data derived from the dense fraction (specific gravity >2.95) of pooled human dental enamel (Young and Mackie 1980). These refinements did not include CO_3^{2-} ions and had equally spaced O atoms along the hexad axis at $z = 0.0, 0.10, 0.2$ or $z = 0.05, 0.15, 0.25$ whose occupancies were refined, instead of an OH^- ion, to represent scattering density along this axis. The structure was very similar to hydroxylapatite, but lattice parameters, $a = 9.441(2)$ and $c = 6.878(1)$ Å, showed the well-known differences from hydroxylapatite ($a = 9.4176$ and $c = 6.8814$ Å, Elliott 1994). Clear evidence exists for a difference in the scattering density distribution along the hexad axis because enamel showed a single maximum in X-ray scattering between $z = 0.1$ and $z = 0.15$ that was not seen with the neutron data. It was suggested that this electron density resulted from H_2O in some orientational disorder and the known small quantity of Cl^- ions

*E-mail: r.m.wilson@mds.qm.ac.uk

0003-004X/99/0009–1406$05.00

TABLE 1. Enamel unit-nit cell contents deduced from chemical analyses, hydroxyl from charge balance

Formula	Reference
$Ca_{9.48}Mg_{0.18}Na_{0.11}(PO_4)_{5.67}(CO_3)_{0.45}(OH)_{1.54}$	Hendricks and Hill (1942)
$Ca_{9.26}(HPO_4)_{0.22}(CO_3)_{0.5}(PO_4)_{5.63}(OH)_{1.26}$*	Aoba and Moreno (1992)
$Ca_{9.23}Na_{.26}K_{.03}(PO_4)_{5.53}(CO_3)_{.47}(OH)_{1.15}Cl_{.06}F_{.01}$	Driessens (1978)
$Ca_{8.856}Mg_{.088}Na_{.292}K_{.010}(PO_4)_{5.312}(HPO_4)_{.280}(CO_3)_{.407}(OH)_{.702}Cl_{.078}(CO_3)_{.050}$†	Elliott (1997)

* Late mature porcine enamel.

† Based on chemical analyses of Little and Casciani (1966), except HPO_4, which comes from Arends and Davidson (1975). Water probably occupies hexad axis sites and possibly other sites.

partially substituting for OH^- ions. R_{wp} for both the neutron and X-ray refinements were in the range 25.5 to 27.4%. Michel et al. (1995) used Rietveld analysis of X-ray data (R_{wp} between 8.04 and 10.4%) to study changes in the CO_3^{2-} environment during fossilization of *Cervus elaphus* (red deer) tooth enamel. The CO_3 content and lattice parameters of the samples varied from 4.13 wt%, a = 9.4468(2) and c = 6.8880(2) Å (modern) to 4.84 wt%, a = 9.4410(2), c = 6.8871(2) Å (oldest fossil). P-O1, P-O2, P-O3 distances (precision ±0.001 Å) varied from 1.515, 1.561, and 1.500 Å (modern) to 1.512, 1.579, 1.476 Å (oldest fossil). Thus the P-O1 distance was shorter than in Holly Springs hydroxylapatite (1.537 Å) and did not change significantly with CO_3 content. The P-O2 distance was larger (hydroxylapatite 1.545 Å) and increased with CO_3, conversely P-O3 was shorter (hydroxylapatite 1.529 Å) and decreased. The occupancies (with reported values corrected for symmetry) of O1, O2, O3, and P for modern enamel were 1.12(2), 1.04(2), set to unity, and 0.894(10), respectively. For the oldest fossil, they were 1.08(2), 1.04(18), set to unity, and 0.884(10), respectively. IR studies indicated that the increase in CO_3 during fossilization was mainly associated with an increased replacement of PO_4^{3-} by CO_3^{2-}, thus it was concluded that this was the origin of the differences in P-O distances from those in Holly Springs hydroxylapatite. However, the P occupancies do not seem to reflect an increase in CO_3^{2-} replacing PO_4^{3-} (there was no discussion of occupancies given by the authors). Michel et al. (1995) also observed an electron density distribution along the hexad axis similar to that of Young and Mackie (1980).

Structural work on dahllite and francolite, carbonate-containing apatites containing under and over 1 wt% F respectively, has been reviewed (Elliott 1994). Though there seems to have been little investigation of dahllite, the closest analogue of enamel, many studies of lattice parameter changes with CO_3 content and chemical analyses of francolite have led to the belief that CO_3^{2-} replaces PO_4^{3-} ions in the lattice with charge balance maintained principally by replacing Ca^{2+} with Na^+ ions. Polarized IR spectra show that the normal to the plane of the CO_3^{2-} ion makes an angle of 37 ± 4° to the c-axis, which is close to 35.3°, the corresponding angle for the inclined face of the PO_4 tetrahedron (assumed to be regular) formed by O1, O2, and O3. Thus, it seems that the positions of these three O atoms form the location for the CO_3^{2-} ion. Perdikatsis (1991) has reported Rietveld analyses of francolite (4.8 wt% CO_2) before and after heating at various temperatures to 1200 °C at which temperature it decomposes to fluorapatite. Reported parameters (Å) for natural and after heating at 1200 °C (in brackets) were: a = 9.3207(5) [9.3708(5)], c = 6.8947(5) [6.8880(5)], P-O1 = 1.496 [1.535], P-O2 = 1.490 [1.553], and P-O3 = 1.565 [1.545]. Thus P-O1 and P-O2 were substantially shorter than in fluorapatite, but P-O3 was slightly longer, a pattern different from that observed in *Cervus elaphus* enamel (above). The occupancies (reported occupancies corrected for symmetry) of O1, O2, O3, and P were 0.902(28), 0.986(24), set to unity, and 0.788(18) [after heating: 0.984(20), 0.998(8), set to unity, and 0.992(16)], respectively. The change in bond lengths and P occupancy were taken as evidence for the partial replacement of PO_4^{3-} by CO_3^{2-} ions.

In summary, there is chemical and IR evidence for the replacement of PO_4^{3-} by CO_3^{2-} ions in mineral and biological apatites. For francolite, there is also clear evidence for this substitution from P occupancies. However, changes in apparent P-O bond lengths are inconsistent. The aim of the present research was to use detailed Rietveld X-ray refinements of four synthetic apatites as a basis for similar refinements of unpooled human dental enamel. Specifically, the intention was to determine the differences in apparent PO_4^{3-} ion geometry and occupancies from hydroxylapatite, and to determine how charge balance was maintained when CO_3^{2-} replace PO_4^{3-} ions.

MATERIALS AND METHODS

Preparation of apatites

Prep. 63b was prepared (Elliott 1964), following Hayek and Stadlemann (1955), by adding a solution of ammonium phosphate to a calcium nitrate solution (both at pH 12) with Ca/P mole ratio of 10/6. The solution was boiled for 10 minutes, filtered, and the apatite washed and dried at 1000 °C in air for 5 h. The analysis (wt%) was: CaO 55.68%; P_2O_5 42.32%; CO_2 < 0.1; H_2O (by difference) 2.00 (theoretical 55.79, 42.39, nil, and 1.80, respectively). H6G was prepared via the reaction of a vigorously stirred aqueous slurry (~80 °C for 20 h) of calcite ($CaCO_3$) and $CaHPO_4$ with the Ca/P mole ratio of 10/6. X-ray diffraction showed only apatite, without detectable calcite. IR and chemical analysis indicated that the apatite contained 4.3 wt% carbonate. Some H6G was heated at 1100 °C for 20 h in air (H6M) and some at 1100 °C for 20 h under a rotary pump vacuum (H6L). Neither Prep. 63b, H6L, nor H6M showed significant impurities by X-ray diffraction at the <1 wt% level. IR showed no significant amounts of CO_3 (strongest CO_3 band at 1410–1460 cm^{-1} barely visible above the noise) and only a weak OH stretch band (3572 cm^{-1}) in H6L, but H6M had a strong stretch comparable to that in Prep. 63b (Fig. 6.1 in Elliott 1964).

Enamel samples

Powdered human enamel samples (~5 mg) were collected from sound natural surfaces of six extracted permanent teeth. The teeth were ground with a dental bur under ethyl alcohol to avoid local heating (>200 °C) at which temperature the mineral structure is irreversibly changed.

TABLE 2. Positional parameters determined from Rietveld analyses $\times 10^4$

Sample	Ca1z	Ca2x	Ca2y	Px	Py	O1x	O1y	O2x	O2y
Holly Springs*	15(1)	2468(2)	9934(1)	3987(2)	3685(1)	3284(2)	4848(2)	5873(2)	4651(2)
H6L	7(6)	2426(3)	9904(4)	3948(4)	3657(4)	3270(9)	4849(9)	5791(9)	4618(9)
H6G	21(4)	2478(2)	9917(3)	3995(3)	3691(3)	3319(6)	4862(6)	5806(7)	4614(7)
H6M	17(4)	2467(2)	9933(2)	3979(3)	3678(3)	3275(6)	4844(6)	5860(6)	4649(6)
Prep.63b	14(3)	2469(2)	9931(2)	3984(2)	3679(2)	3273(4)	4848(4)	5852(4)	4635(4)
RC1	14(6)	2450(3)	9895(4)	3987(5)	3697(4)	3317(9)	4864(9)	5752(9)	4555(9)
RC7	42(6)	2457(3)	9896(4)	3982(5)	3686(4)	3283(8)	4859(8)	5754(8)	4551(8)
RC8	24(6)	2442(3)	9880(4)	3975(6)	3668(5)	3254(9)	4863(10)	5684(9)	4542(9)
RE1	41(6)	2437(3)	9888(4)	3969(5)	3669(4)	3317(8)	4902(9)	5739(8)	4562(8)
RE2	24(7)	2452(4)	9905(5)	3977(5)	3696(5)	3327(9)	4875(10)	5779(9)	4602(9)
RFP	7(5)	2463(3)	9893(4)	3998(5)	3688(4)	3286(8)	4869(9)	5772(9)	4558(9)
RFB	26(4)	2460(2)	9899(3)	3991(3)	3694(3)	3337(6)	4875(7)	5804(6)	4600(6)
RGP	26(4)	2471(3)	9909(3)	3996(4)	3692(3)	3311(6)	4857(7)	5805(7)	4599(7)
RGB	21(4)	2464(2)	9907(3)	3992(3)	3692(3)	3322(6)	4864(6)	5802(6)	4608(6)
RHP	19(5)	2470(3)	9912(3)	3999(4)	3691(4)	3299(7)	4865(7)	5781(8)	4568(7)
RHB	15(4)	2476(3)	9914(3)	3999(4)	3693(3)	3301(6)	4847(7)	5796(7)	4590(7)
RQ1	19(6)	2448(4)	9879(4)	4025(6)	3693(5)	3310(9)	4880(10)	5821(10)	4574(10)
Mean†	23	2457	9898	3991	3688	3305	4868	5774	4576
σ_{n-1}†	10	12	12	15	10	23	14	38	22

Notes: Parameters fixed by symmetry are Ca1x at 1/3, Ca1y at 2/3, $O_{OH}x$ and $O_{OH}y$ at 0 and all others at 1/4. Hz fixed at 0,0,0.0608, standard deviation for last figure given in brackets. Space group for all samples is $P6_3/m$.

* Single crystal determination of natural hydroxylapatite from Holly Springs (Sudarsanan and Young 1969) by neutron scattering, lattice parameters by X-rays, a = 9.424(4) and c = 6.879(4) Å.

† Means and standard deviations calculated for the n = 12 enamel samples.

X-ray diffraction powder data collection

A 1500 W sealed tube with a Cu target (25 mA and 40 kV) was used with a Ge 111 monochromator to give Cu$K\alpha_1$ radiation (λ = 1.5406 Å). Diffraction patterns were collected with an INEL CPS-120 (Ballon et al. 1983; Evain et al. 1993) curved position sensitive detector that allows simultaneous data collection in 4096 bins over 1° to 121° in 2θ. The geometry used was a fixed flat plate with the incoming monochromatic beam striking the sample holder at an angle of between 2° to 5°. The sample holder was a (711) cut Si single crystal oriented to minimize the background. The sample holder was rotated about the axis defined by the planar surface of the sample to increase the number of crystallites in differing orientations contributing to the powder pattern, thus obtaining a better powder average.

The INEL CPS-120 geometry differs from the usual Bragg-Brentano geometry for powder diffraction in that the diffraction vector is not fixed perpendicular to the sample surface but, of course, still bisects the incident and diffracted X-ray beams. Consequently, in Bragg-Brentano geometry, all orders of diffraction for a given *hkl* plane will come from the same crystallites, as only they will have the right orientation to diffract. With the INEL CPS-120, change of the diffraction vector with 2θ value means that, for example, crystallites oriented to diffract 100, will not be the same crystallites that diffract 200. Consequently, the INEL geometry samples the orientation distribution of the powder more effectively than Bragg-Brentano instruments.

Generally, 1–3 mg samples were used, but smaller quantities have been used successfully. Samples were loaded onto the Si sample holder by grinding in acetone and applying the dilute slurry to the surface of the sample holder, thus ensuring a smooth and uniform covering. The patterns were collected for 60–120 or 1000–1080 minutes, depending on the amount of sample or time available. For the 60–120 minute runs, the most intense peak height was $>10^4$ counts; for the 1000–1080 minute runs, the most intense peak height was $>10^5$ counts. Patterns were corrected for any offsets using calibration curves produced from lead nitrate patterns usually run before and after each sample, and always of similar quality to the sample data sets. Consequently, the accuracy of the calibrated data is related to the accuracy of the lead nitrate calibration data. The calibration curves were a least squares spline fitted to the differences between the measured and calculated (using a = 7.8586 Å at ~20 °C, Nowotny and Heger 1986) positions of the 27 most intense lead nitrate peaks between 19° and 117° in 2θ. As a result of the calibration, the number of points was reduced slightly by the calibration software from the original 4096 bins. (The nominal software generated separation is 0.029°.)

Rietveld analysis

The program GSAS (Larson and Von Dreele 1986) was used for Rietveld refinement, treating the data as if it came from Bragg-Brentano geometry, rather than the fixed flat plate geometry actually used. Two possible objections to this approach are first, the differing forms of absorption correction, and second, the fixed flat plate's differing (and greater) sensitivity to shifts normal to its surface. As both the absorption (μ~270 cm^{-1} for apatite) and estimated sample thickness (~20 μm) are small, and the known shift of the sample holder (measured with a vernier microscope) was of the order of a few micrometers, Bragg-Brentano geometry could be used in the refinement without introducing any significant perturbations to the structural model. The background was modeled using Chebyschev polynomials of the first kind. The March-Dollase model for preferred orientation made a significant improvement for some of the refinements although the coefficients indicated very little preferred orientation. The best peak shape was found to be a Lorentzian with slight asymmetry. Starting atomic parameters for all refinements (including the z-axis models) came from the refinement performed with neutron data in $P6_3/m$ of Sudarsanan and Young (1969). Occupancy, atom position, unit cell, peak profile, 2θ zero, pre-

TABLE 2—*Extended*

O3x	O3y	O3z	O(H)z
3437(2)	2579(1)	702(2)	1950(7)
3417(7)	2578(7)	711(7)	1837(34)
3437(5)	2593(5)	697(5)	1906(22)
3424(5)	2577(4)	685(5)	1999(21)
3415(3)	2565(3)	690(3)	1917(13)
3427(7)	2587(7)	734(7)	1880(29)
3359(7)	2526(6)	699(6)	1881(27)
3445(7)	2604(6)	697(7)	1747(25)
3398(7)	2567(6)	693(7)	1857(25)
3364(8)	2532(8)	716(8)	1881(32)
3444(6)	2599(6)	716(6)	1748(22)
3414(5)	2579(5)	704(5)	1803(18)
3408(5)	2577(5)	718(5)	1818(17)
3399(5)	2565(4)	697(4)	1851(17)
3431(5)	2590(5)	713(5)	1785(19)
3436(5)	2592(5)	706(5)	1771(17)
3437(7)	2611(6)	737(7)	1817(25)
3413	2577	711	1820
29	26	14	50

ferred orientation, and background parameters were allowed to vary. The anisotropic thermal parameters and the occupancy of Ca1, set at the stoichiometric value (unity), were kept constant throughout the refinement. Refinements were made for all data sets with a single O and H atom in the *z*-axis channel (Table 2). Second and third refinements to model the *z*-axis channel scattering density were then carried out using all four of the synthetic sample data sets, and four of the enamel data sets. In the second set of refinements, scattering along the *z*-axis was modeled by refining the occupancies of equally spaced O atoms on the axis at $z = 0.0, 0.10, 0.2$, and in the third set at $z = 0.05, 0.15, 0.25$, instead of the O and H, following Young and Mackie (1980).

R_{wp} comparison

R_{wp} values should not be taken at face value when comparing the quality of structural refinements performed with data from different machines. The actual data and the models should be examined directly, or with the help of difference plots. This is especially true if the data are collected on diffractometers with different geometries. In particular, R_{wp} values improve, as the background increases. The lack of a set of diffracted beam slits on the INEL diffractometer (compared with a Bragg-Brentano machine) means that the INEL background is more intense for a given peak intensity. This makes comparison of our work with previous work difficult. However, without being able to examine all the previous refinements in detail, R_{wp} values are the only available means of comparison.

As an aid to comparing our refinements with those from Bragg-Brentano geometry machines, the NIST standard hydroxylapatite SRM2190 (Anonymous 1997) was run on the INEL CPS-120 diffractometer and a Bragg-Brentano Siemens D5000 diffractometer. The INEL data was collected for 3840 minutes and had a maximum intensity of 55.1×10^4 counts. The Siemens data took 1020 minutes and had a maximum intensity of 0.95×10^4 counts. The simplest, and least biased, way of modeling the increased background of the INEL machine was to assume that the extra background was additive and constant with angle. The data were scaled to one another using a linear least squares fit of the form

$$y(\text{INEL}) = A y(\text{Siemens}) + C,$$

where the y values are the respective counts. A and C were 56.18 and 7553, respectively, and, on average, the y(INEL) intensities were within about 7% of the modeled Ay(Siemens)+C values. To derive a data set roughly approximating to a Bragg-Brentano geometry data set of similar quality to the INEL data, 7553 counts were subtracted from each INEL intensity measurement.

The three data sets (Siemens, INEL, high intensity Bragg-Brentano approximation) were used in refining the SRM2190 structure, starting from that in Sudarsanan and Young (1969). The three refinements gave positional parameters identical to within 0.002 and occupancies to within 0.02 with the exception of H (0.5 ± 0.12). The R_{wp} values were 9.47% (Siemens), 3.76% (INEL), and 5.73% for the high intensity Bragg-Brentano approximation. This tells us that the reduction in R_{wp} due to the higher background in the INEL data is around 2%. The rest of the difference is probably due to the better statistics of the INEL data, or perhaps a better peak shape model in the refinement. The enamel data set collection time was shorter than for SRM2190. This may mean that the reduction in R_{wp} from the increased background is larger than 2%, but it is thought unlikely to be greater than 3%.

Calculation of unit-cell contents of enamel

The structural model used in the refinements contains only Ca, P, O, and H. The presence of CO_3 and trace quantities of Mg and Na present in the samples would unpredictably distort both the occupancies and thermal parameters for Ca, P, O, and H obtained by simultaneous refinement of these parameters as they are known to be correlated. The neutron anisotropic thermal parameters from Holly Springs hydroxylapatite (Sudarsanan and Young 1969) were therefore chosen as a good static model for the Ca, P, O, and H thermal parameters in enamel, while only the occupancies were refined. This procedure introduces small errors in the site occupancies. Further small errors in occupancies might arise from the (slight) dependence of scattering factors on the atomic environment. Such errors were corrected for by using the occupancies from the synthetic apatite refinements to calculate correction factors (given under Results) which, when multiplied by the experimental occupancies from stoichiometric hydroxylapatite, would give the correct unit-cell contents. Four different apatites were used to check that the correction factors were consistent and were, as far as possible, not biased toward individual structures. Based on the assumption of stoichiometric Ca/P ratios, correction factors for Ca2 and P were calculated from the mean occupancies of the four samples. H6G was omitted from the calculation of the factors for O1, O2 and O3 because of its CO_3 content. Only H6M and Prep. 63b were used for the O_{OH} factor because H6L would have lost OH^- ions, and H6G was likely to contain H_2O in the hexad channels. Occupancies from the Rietveld refinements of the enamel apatites were multiplied by

TABLE 3. PO_4 bond lengths (Å) and volume (Å^3)

Sample	P-O1	P-O2	P-O3*	PO_4 vol
Holly Springs†	1.537(3)	1.545(3)	1.529(2)	1.853(3)
H6L	1.543(9)	1.502(8)	1.514(6)	1.79(1)
H6G	1.528(6)	1.481(5)	1.532(4)	1.792(9)
H6M	1.541(5)	1.534(5)	1.538(4)	1.864(9)
Prep.63b	1.549(4)	1.525(3)	1.543(2)	1.872(6)
RC1	1.525(10)	1.447(7)	1.518(5)	1.73(1)
RC7	1.549(9)	1.450(6)	1.562(4)	1.83(1)
RC8	1.581(10)	1.396(7)	1.513(5)	1.73(1)
RE1	1.569(10)	1.449(7)	1.537(5)	1.81(1)
RE2	1.519(11)	1.476(7)	1.555(5)	1.82(1)
RFP	1.566(9)	1.454(7)	1.517(4)	1.77(1)
RFB	1.521(7)	1.486(5)	1.538(4)	1.802(9)
RGP	1.531(7)	1.481(5)	1.523(3)	1.792(9)
RGB	1.525(6)	1.480(5)	1.546(3)	1.815(8)
RHP	1.551(8)	1.460(6)	1.525(4)	1.78(1)
RHB	1.534(7)	1.473(5)	1.529(3)	1.785(9)
RQ1	1.574(11)	1.471(8)	1.503(5)	1.77(1)
Mean‡	1.545	1.460	1.531	1.787
σ_{n-1}‡	0.023	0.024	0.017	0.033

* Repeated by symmetry.
† Bond lengths and tetrahedron volumes for natural hydroxylapatite calculated from positional parameters from neutron data in Sudarsanan and Young (1969).
‡ Means and standard deviations calculated for the n = 12 enamel samples.

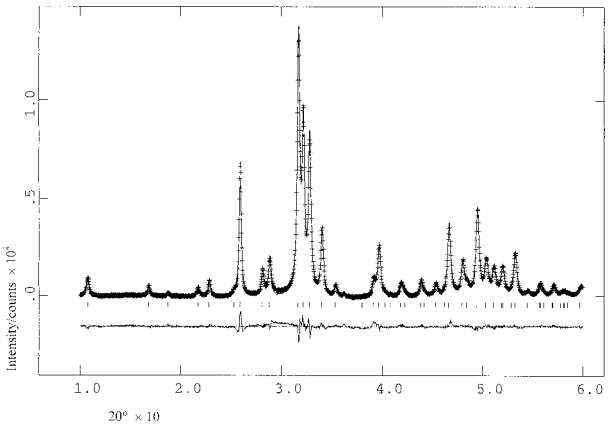

FIGURE 1. Part of the experimental (+ symbols) and calculated (solid line) powder pattern (R_{wp} = 5.2%) for RGB. The lower trace is the difference between observed and calculated patterns, and tick marks in the middle are the positions of lines calculated from refined lattice parameters.

these factors to give unit-cell contents. Another factor was applied to correct for the assumption made in the refinements that all the cations in enamel are Ca^{2+} ions, whereas Na^+ and Mg^{2+} ions are also present. Thus the occupancies of the two cation sites were apportioned to Ca^{2+}, Na^+, and Mg^{2+} ions so that their respective mole percentages were 95.78, 3.27, and 0.95% (derived from chemical analyses of Little and Casciani 1966) and the X-ray scattering for each site remained unchanged (based on ratios of ion scattering at $\theta = 32°$, $\sin\theta/\lambda = 0.30$). Thus an occupancy of 1 for "Ca^{2+}" was replaced by $0.984Ca^{2+} + 0.022Na^+ + 0.005Mg^{2+}$ (total cations 1.011 and charge +2.000). The total number of cations per unit cell in Ca1 sites was preserved at four, by dividing all the occupancies by 1.011.

RESULTS

The typical fit between the calculated and observed powder patterns for the enamel and synthetic samples is illustrated in Figure 1 for an enamel sample for which R_{wp} was 5.2%. Some enamel samples had one or two very weak lines in the 2θ angular range 35–39°, not ascribable to apatite, but later found to be due to the sample holder. Extra reflections also appeared in synthetic apatite Prep. 63b and H6M, but in these cases they indicated a monoclinic space group $P2_1/b$ as found in stoichiometric hydroxylapatite (Elliott 1994). Although refinements could be done with $P2_1/b$ symmetry, those presented here are for $P6_3/m$ to enable direct comparison with enamel.

Positional parameters for the synthetic apatites and enamel samples are given in Table 2 and P-O bond lengths and PO_4 tetrahedral volumes in Table 3. Lattice parameters and occupancies for the synthetic apatites are given in Table 4, and lattice parameters and unit-cell contents calculated from occupancies for the enamels in Table 5 (columns 3–11). The correction factors calculated from the occupancies in Table 4 and used for Table 5 are 0.995, 1.024, 0.974, and 0.883 for Ca2, P, O_{OP}, and O_{OH}, respectively. The standard deviations of

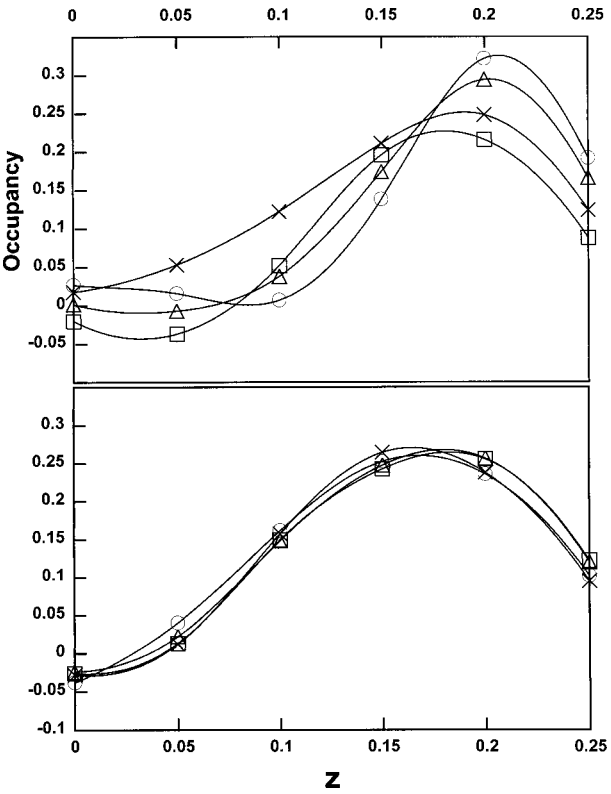

FIGURE 2. Occupancies of dummy O atoms along hexad axis from pairs of refinements. Upper section, synthetic apatites (open triangle = Prep. 63b, open circle = H6M, × = H6G, open box = H6L) and lower figure, enamel (open triangle = RGP, open circle = RFB, × = RFP, open box = RGB). Occupancies from GSAS have been halved to account for the two refinements contributing to each plot (those for the mirror plane at z = 1/4 and center of symmetry at z = 0 have been further divided by two as GSAS only generates two atoms per unit cell for these sites, whereas four are generated for the other sites).

TABLE 4. R_{wp}, lattice parameters, occupancies,* and densities for the synthetic apatites

Sample	R_{wp}(%)	*a* (Å)	*c* (Å)	Ca2	P	O1	O2	O3	O_{OH}	H	ρ(g/cm³)†
H6L	9.5	9.4081(5)	6.8887(4)	1.007(5)	0.992(7)	1.007(10)	0.999(11)	1.017(9)	0.465(14)	0.082(135)	3.160
H6G	8.1	9.4394(4)	6.8861(3)	0.978(4)	0.931(5)	1.020(7)	1.013(8)	1.007(7)	0.518(10)	2.023(93)	3.120
H6M	10.0	9.4172(1)	6.8799(1)	1.022(4)	0.993(5)	1.026(8)	1.016(8)	1.052(6)	0.553(9)	0.937(88)	3.230
Prep.63b	6.0	9.4232(2)	6.8833(2)	1.014(2)	0.990(3)	1.027(5)	1.021(5)	1.045(4)	0.580(7)	0.639(63)	3.216

* Scaled so that Ca(1) has an occupancy of 1, so that stoichiometric occupancies for other sites are 1, except O(H) and H, which are 0.5 because the OH^- ion is in two-fold disorder. Space group for all samples is $P6_3/m$.
† From lattice parameters and unit cell contents based on above occupancies.

the occupancies of the enamel refinements used in Table 5 were similar to those given for the synthetic apatites in Table 4, namely 0.5 to 0.7%, 0.7 to 1%, 0.7 to 1%, 1.3 to 1.6%, and 12 to 15% for Ca2, P, O, O_{OH}, and H, respectively.

Distributions of scattering along the hexad axis for the synthetic and four of the enamel apatites are given in Figure 2.

DISCUSSION

Comparison of experimental and calculated patterns shows a very good fit (Fig. 1), indicating that precise structural parameters should be obtained from the refinements. This is confirmed by the agreement of the positional parameters (Table 2), and PO_4 bond lengths and volumes (Table 3) from the Rietveld refinements for the stoichiometric hydroxylapatites (H6M and Prep. 63b) with the neutron single crystal study (Holly Springs). Standard deviations of the positional parameters for H6M and Prep. 63b are about twice those for Holly Springs and agree within two standard deviations (a little larger for some O atoms). The PO_4 bond lengths and volumes agree within two standard deviations (a little larger for P-O2). Parameters for the other two synthetic apatites (H6L and H6G) are generally different from the single-crystal values (often 10 standard deviations, and more for P-O2), as would be expected for slightly non-stoichiometric apatites. H6L probably lost OH^- ions through the heating in vacuum, which is consistent with its reduced *a*-axis parameter (Table 4), as found in oxyapatite (Trombe and Montel 1971), and its low occupancy for O_{OH} (Table 4); and H6G contains CO_3 and H_2O, which is reflected in its increased *a*-axis, as is found in the enamel apatites.

In contrast, occupancies for Ca2, P, O_{OP}, and O_{OH} for the synthetic apatites (Table 4) show small, but consistent, departures from stoichiometric values. Densities calculated from the occupancies for stoichiometric hydroxylapatites H6M and Prep. 63b (3.230 and 3.216 g/cm³, respectively) are also higher than for stoichiometric hydroxylapatite (3.156 g/cm³, Elliott 1964). These differences could easily arise from small errors in the atomic scattering factors, temperature factors or the absence of absorption corrections. Thus, as described above, correction factors were calculated to apply to the occupancies when calculating the unit-cell contents of the enamel apatites.

Differences in the mean positional parameters of enamel apatite (Table 2) from those for single-crystal Holly Springs hydroxylapatite (Holly Springs, Table 2) are all <0.004, except for O2*x* (–0.0099), O2*y* (–0.0075), and OHz (–0.0130). The most noticeable differences in the PO_4 tetrahedron of enamel apatite from hydroxylapatite (Holly Springs, Table 3) are marked reductions in the P-O2 bond length and tetrahedron volume. For P-O1, P-O2, P-O3, and the volume, the differences are: +0.55, –5.49, +0.14, and –3.59%, respectively. The fact that P-O2 differs most is consistent with the change in the O2x and O2y parameters noted above. Young and Mackie (1980) did not comment on differences in PO_4 tetrahedron volume in enamel apatite from hydroxylapatite. Their P-O bond lengths for enamel apatite were rather scattered between refinements, with means (based on all refinements) for P-O1, P-O2, and P-O3 of 1.592, 1.472, and 1.564 Å, respectively. These values give differences from Holly Springs hydroxylapatite of +3.61, –4.70, and +2.26%, respectively. The mean volume difference from hydroxylapatite calculated from Young and Mackie's parameters is +2.37%. Young and Mackie's results are therefore only in part consistent with the present ones; this can probably be explained by their much larger R_{wp} values. Michel et al. (1995) reported bond lengths (see Introduction) for modern *Cervus elaphus* enamel apatite that give differences from Holly Springs hydroxylapatite for P-O1, P-O2, and P-O3 of –1.43, +1.03, and –1.90%, respectively. The difference in the PO_4 volume from hydroxylapatite calculated from Michel et al.'s parameters is –3.80%. Thus, Michel et al.'s results are noticeably different from the present ones, except for the volume difference. Michel et al.'s R_{wp} values are about 3% higher than in the present work (8–10% vs. 5–8%). This would normally indicate that our model was an improvement on the previous one, but from the comparison of refinements performed on SRM2190 discussed earlier, most of this may be attributable to the higher background from the INEL geometry. Both the work of Michel et al. and the present are internally more consistent than the observed differences between them. Michel et al. studied a different species (red deer as opposed to human), but their chemical analyses do not suggest any significant differences in composition from human enamel. This is borne out by unit-cell contents deduced from the X-ray results (see later). However, a slight increase of 0.04 Å in P-O bond lengths seen in Ca-deficient apatites containing Na has been ascribed to HPO_4^{2-} ions (Jeanjean et al. 1994). As enamel contains HPO_4^{2-} ions (Table 1), it could be that red deer and human enamel have different HPO_4^{2-} contents; these would not have been detected by Michel et al.'s analyses. The magnitude of possible bond length changes can be gauged from molecular orbital calculations (Salinas et al. 1997), which give P-O(H) bonds 13–15% longer than unprotonated P-O bonds (with a substantially smaller increase in the presence of water). There is also some evidence that differences in observed P-O bond lengths between enamel and Holly Springs hydroxylapatite are not entirely determined by CO_3^{2-} replacing PO_4^{3-} ions. Michel et al. observed that, although the P-O1 bond length in modern red deer enamel was 0.022 Å less than in hydroxylapatite, it did not decrease further with an increased replacement of PO_4^{3-} by CO_3^{2-} ions in fossil samples, whereas the other P-O bond lengths did change.

TABLE 5. R_{wp}, lattice parameters, unit cell contents* and densities for enamel samples

Sample	R_{wp}(%)	*a* (Å)	*c* (Å)	Ca2†	P,*p*′‡	O1	O2	O3	O_{OH}	H
RC1	7.1	9.4623(19)	6.8863(14)	5.68	5.50	5.45	5.72	10.70	1.90	2.33
RC7	7.4	9.4512(25)	6.8803(18)	5.68	5.58	5.34	5.98	10.51	2.08	4.04
RC8	7.2	9.4343(22)	6.8681(16)	5.58	5.23	5.45	6.18	11.23	2.26	0.92
RE1	7.8	9.4564(17)	6.8821(12)	5.71	5.54	5.23	5.86	10.38	2.09	3.50
RE2	10.0	9.4598(18)	6.8865(13)	5.69	5.59	5.35	5.97	10.22	1.90	3.17
RFP	4.9	9.4592(17)	6.8816(12)	5.61	5.47	5.48	5.69	11.06	2.18	2.47
RFB	4.7	9.4586(11)	6.8811(8)	5.72	5.69	5.45	5.79	10.81	2.01	3.56
RGP	5.2	9.4554(9)	6.8835(7)	5.71	5.64	5.59	5.86	10.88	2.12	3.22
RGB	5.2	9.4506(9)	6.8780(7)	5.75	5.69	5.63	5.82	11.05	2.05	4.50
RHP	4.6	9.4586(13)	6.8809(10)	5.69	5.54	5.55	5.73	11.02	2.11	2.93
RHB	4.7	9.4616(11)	6.8819(8)	5.69	5.68	5.62	5.75	11.18	2.15	2.19
RQ1	4.9	9.4584(19)	6.8808(13)	5.64	5.26	5.56	5.73	10.86	2.05	4.96
Mean	—	9.4555	6.8809	5.68	5.53	5.48	5.84	10.83	2.07	3.15
σ_{n-1}	—	0.0076	0.0047	0.05	0.15	0.12	0.14	0.32	0.10	1.10

* From occupancies corrected with factors from synthetic apatite refinements and scaled so that there are 4 cations ($3.892Ca^{2+} + 0.087Na^{+} + 0.021Mg^{2+}$) in Ca1 sites per unit cell. Space group for all samples is $P6_3/m$.
† The value attributes the entire scattering to Ca^{2+}, thus each Ca^{2+} is to be replaced by $0.984Ca^{2+} + 0.022Na^{+} + 0.005Mg^{2+}$.
‡ *p*′ is the directly calculated number of P atoms without regard to contribution from C atoms.
§ O_T = O1 + O2 + O3.
|| Assuming that *p* + *c* = 6 and 25% of *c* contributes to scattering of *p*, where *p* and *c* are the number of P and C atoms per unit cell deduced from *p*′ (see text for further details).
O_T - (4*p* + 3*c*) i.e., number of O atoms found in tetrahedral sites not accounted for by requirement of P and C atoms for O atoms.
** Monovalent anions in hexad axis from charge balance requirement taking into account Na^{+} and Mg^{2+} ions.
†† From lattice parameters and unit cell contents.

The differences in P-O1, P-O2, and P-O3 bond lengths in francolite from fluorapatite (Perdikatsis 1991, see Introduction) are –2.54, –4.06, and +1.29%, respectively. The volume difference for francolite from fluorapatite is –4.70%. This pattern of change is rather similar to that found here (+0.55, –5.49, +0.14, and –3.59%, respectively), except for P-O1. Exact identity would not be expected because the *a*-axis of francolite is less than in fluorapatite, whereas enamel apatite has a larger *a*-axis than hydroxylapatite. Thus, apparent P-O bond length changes seem not to be dominated by replacing PO_4^{3-} by CO_3^{2-} ions, but are also affected by other lattice changes. However, volume changes for comparable amounts of CO_3^{2-} replacing PO_4^{3-} ions are very consistent between francolite, modern *Cervus elaphus* and human enamel apatite (–4.70, –3.80, and –3.59%, respectively).

Like enamel apatite, both H6L and H6G have a reduced P-O2 bond and PO_4 volume compared to Holly Springs hydroxylapatite (Holly Springs, Table 3). For H6G, this could be caused by the CO_3 that it contains, but this explanation cannot apply to H6L, as it is free of CO_3. Although this exception applies to only one sample, the conclusion must be that the reduced P-O2 bond length and PO_4 volume in enamel apatite compared with stoichiometric hydroxylapatite cannot be taken as proof of the partial replacement of PO_4^{3-} ions by CO_3^{2-} ions, but only that it is consistent with it.

When the density is not accurately known, as for enamel apatite crystals, X-ray diffraction or chemical analyses give only relative occupancies in the unit cell, unless some assumption is made. For chemical analyses of apatites, it is usually assumed that all tetrahedral sites are filled. This assumption is not applicable to X-ray studies because occupancies of individual atom sites, rather than polyatomic ion sites, are refined. Thus, Young and Mackie (1980), Perdikatsis (1991), and Michel et al. (1995) assumed that the total number of O3 atoms in the unit cell was 12, the stoichiometric value. This is not entirely satisfactory because O has low X-ray scattering, so this occupancy is subject to proportionately more error. Further, this assumption results in more than six ions in tetrahedral sites because each CO_3^{2-} ion contributes less than one O atom to O3. There are two reasons for this, first, the ion contributes only 1/2O to O3 as it is in disorder about the mirror plane at $z = 1/4$, and second, this O atom will not be centered on the refined position of O3 because the CO_3^{2-} ion is smaller than the PO_4^{3-} ion. As inspection of the occupancies for enamel apatite showed clearly that the ratio of Ca1/Ca2 was greater than in stoichiometric hydroxylapatite, it was decided to analyze the results in terms of the hypothesis that all the Ca1 sites were filled, with vacancies in Ca2 sites. This distribution of Ca and vacancies is also seen in Rietveld refinements of Ca-deficient apatites containing Na (Jeanjean et al. 1994) and without Na (Rodrigues-Lorenzo et al. 1997).

No attempt was made at this stage to determine the position and number of CO_3^{2-} ions per unit cell directly from the X-ray results. However, there is further support for the presence of CO_3^{2-} in PO_4^{3-} sites as the mean number of P atoms per unit cell calculated directly from the observed P occupancies (Table 5, column 6), is 5.53, substantially less than 6. In the following discussion, *p*′ refers to the directly calculated number of P atoms per unit cell (Table 5, column 6), *p* and *c* to the number of P and C atoms per unit cell deduced from *p*′ (Table 5, columns 13 and 14, respectively); the ~10% of the CO_3^{2-} ions that are in the hexad axis and the small amount of HPO_4^{2-} ions are ignored. An estimate of *c* can be made assuming that the tetrahedral sites are filled with PO_4^{3-} plus CO_3^{2-} ions, that is to say that $p + c = 6$, and a further assumption about the contribution of C to the scattering of P. If this further assumption is that the contribution of C is nil, $p = p'$ so that $c = 6 - p'$, but if C contributes to the P scattering, *c* and *p* will increase and decrease, respectively. For any given contribution, *p* and *c* can be calculated from the requirement that the X-ray scattering of *p* and *c* combined is the same as that from *p*′ (based on scattering at $\theta = 32°$, $\sin\theta/\lambda = 0.30$), and that $p + c = 6$. This calculation for 0, 25, and 100% contributions from C, gives mean values of *c* of 0.47, 0.50, and 0.65 atoms per unit cell, respectively. It is un-

TABLE 5—*Extended*

O_T§	p ||	c ||	Δ#	X-**	ρ(g/cm³)††
21.87	5.46	0.54	–1.59	1.82	3.013
21.84	5.55	0.45	–1.71	1.72	3.026
22.85	5.17	0.83	–0.32	1.91	3.000
21.47	5.51	0.49	–2.03	1.82	3.027
21.55	5.56	0.44	–2.01	1.74	3.022
22.22	5.43	0.57	–1.21	1.71	3.000
22.06	5.67	0.33	–1.61	1.68	3.038
22.33	5.62	0.38	–1.28	1.72	3.034
22.49	5.66	0.33	–1.18	1.75	3.051
22.31	5.50	0.50	–1.20	1.79	3.022
22.55	5.66	0.34	-1.11	1.65	3.029
22.15	5.21	0.79	-1.06	1.98	3.000
22.14	5.50	0.50	-1.36	1.78	3.021
0.41	0.17	0.16	0.47	0.10	0.017

likely that C contributes 100% to P and this is confirmed by the fact that c is then clearly too high (compare with Table 1). In fact, it is unlikely that the contribution exceeds 25%, at which level the particular value chosen has little effect on the calculated results. For this reason, only detailed results for 25% are given (Table 5, columns 13 and 14).

The occupancy of O_{OH} in enamel, and other apatites with H_2O or other substitutions in the hexad axis, cannot be determined confidently from a Rietveld refinement because of the distribution of scattering along the hexad axis. However, the occupancy can also be calculated from the charge balance (Table 5, column 16) assuming that ions such as HPO_4^{2-} are absent. This shows a mean deficiency of about 11% from stoichiometric hydroxylapatite. A much larger OH^- ion deficiency is indicated by chemical analyses and charge balance (Table 1) and by the fact that the area of the OH IR band at 3569 cm^{-1} in enamel could increase by ~70% as a result of heating to 400 °C (Holcomb and Young 1980). The smaller deficiency found here could easily arise from an error in the occupancy of one of the major ions.

Neither Young and Mackie nor Michel et al. determined the distribution of scattering along the hexad axis for hydroxylapatite with sets of O atoms, so a direct comparison with enamel apatite could not be made. Distributions for the stoichiometric hydroxylapatites (H6M and Prep. 63b) and enamel apatites (Fig. 2) confirm that those for enamel apatite are indeed significantly wider than for stoichiometric hydroxylapatite. As suggested by Young and Mackie, this is probably due to H_2O and Cl^- ions, but relaxation along the hexad axis of OH^- ions adjacent to OH^- ion vacancies may also contribute significantly. A wider distribution is also seen for the nonstoichiometric H6L and H6G samples (Fig. 2), presumably for similar reasons.

There are two necessary, but not sufficient, conditions for the hypothesis of fully filled Ca1 sites to be valid. First, O_T, the sum of the O1, O2, and O3 atoms, should not exceed 24; Table 5 (column 12) shows that this condition is always met. Second, O_T should be close to the sum of the O atoms associated with the p PO_4^{3-} and c CO_3^{2-} ions, and preferably slightly less because the O atoms from the CO_3^{2-} ions will not contribute fully to O_T as they will not exactly coincide with the refined O positions; Table 5 shows that $O_T - (4p + 3c)$ (Δ in column 15) is about –1.4, so this condition is also fulfilled. Thus the two necessary conditions are met, but this does not prove that the Ca1 sites are filled, though this is most probable. If they are not filled, the unit-cell contents in Table 5 will have to be reduced by a common factor. As it is very improbable that the Ca1 sites could be overfilled, the results in Table 5 are maximum values.

The mean unit-cell contents of enamel apatite in Table 5 can be summarized by the chemical formula $Ca1_{3.89}Na1_{0.09}Mg1_{0.02}Ca2_{5.59}Na2_{0.13}Mg2_{0.03}(PO_4)_{5.50}(CO_3)_{0.50}(OH)_{1.78}$.

The equivalent formula for *Cervus elaphus* enamel calculated following the procedure used for Table 5 from means of the X-ray results and chemical analyses for modern and fossil samples (Michel et al. 1995) is $Ca1_{3.89}Na1_{0.09}Mg1_{0.02}Ca2_{5.65}Na2_{0.13}Mg2_{0.03}(PO_4)_{5.38}(CO_3)_{0.62}(OH)_{2.01}$.

The unit-cell contents deduced for *Cervus elaphus* enamel are in satisfactory agreement with those for human enamel (the identity of occupancies of the Ca1 sites is fortuitous). The mean CO_3 content for the *Cervus elaphus* enamel calculated from individual chemical analyses (Michel et al. 1995) is 4.67 wt%, which gives 0.75 CO_3^{2-} ions per unit cell, consistent with the above formula.

The lattice parameters and unit-cell contents in Table 5 can be used to calculate the densities of the enamel apatite crystals (column 17). These are maxima apart from small increases from any lattice H_2O (each molecule in the unit cell increases the calculated density by ~0.056 g/cm³). The densities (mean 3.021 g/cm³) are all significantly less than calculated for stoichiometric hydroxylapatite (3.156 g/cm³). The density of enamel apatite can also be calculated using unit-cell contents based on chemical analyses (Table 1, last entry) and is 2.99 g/cm³ (Elliott 1997). This is close to the mean of the results in Table 5 (3.021 g/cm³). This agreement appears to be very satisfactory, but it should be recalled that both densities are based on the hypothesis that the scaling factor for the unit-cell contents should be such that one site in the unit cell is completely filled, but no other site is overfilled. In one case, it is the PO_4^{3-} site (chemical analyses) and the other, the Ca1 site (X-ray multipliers); as the analysis of the X-ray results shows, these hypotheses appear to be nearly equivalent. Given this, it could be argued that the consistency between the densities only indicates that the chemical analysis of bulk enamel reflects the chemical composition of the crystal unit cell. This would only be true if enamel apatite were the only, or at least the principal, phase in enamel, and that ions on the surface of the apatite crystals make a minimal contribution to the composition of enamel. It is generally accepted that these two conditions are met, given the reasonably well-crystallized nature of enamel apatite.

Discussion has so far been restricted to mean values for enamel apatite. However, the samples are not expected to be identical because of the known variability in the composition of enamel. The variation in refined parameters over all the data sets, when compared to the standard deviations of the individual refinements, would tend to support this variability. (The stan-

dard deviations of the means in Tables 2, 3, and 5 are generally 2 to 4 times the standard deviations of the individual parameters as calculated from the inverse of the least squares normal matrix.) As the estimated standard deviations from the inverse matrix are minimum possible probable errors, the difference is probably too small to have much significance.

In conclusion, we have obtained detailed information about positions of atoms and occupancies of sites from Rietveld refinements using X-ray data collected from milligram samples of enamel apatite. This provides a sound foundation on which to undertake future chemical, compositional, or structural work. For example, studies of regional variations within and between clinically normal teeth, and changes in enamel mineral during developmental and acquired (e.g., caries, acid erosion) conditions and diagenetic processes.

ACKNOWLEDGMENTS

This work was supported by the Medical Research Council (grant no. G9505593MA). We thank Huda Morgan for the preparation of the synthetic apatites; Iain Gibson of the Interdisciplinary Research Centre in Biomedical Materials at Queen Mary and Westfield College for the Siemens D5000 powder diffractogram of SRM2190.

REFERENCES CITED

Anonymous (1997) SRM2910 Calcium Hydroxyapatite, Certificate Issue date: 3 November 1997, NIST SRM Program, Gaithersburg, MD 20899–2320 U.S.A.

Aoba, T. and Moreno, E.C. (1992) Changes in the solubility of enamel mineral at various stages of porcine amelogenesis. Calcified Tissue International, 50, 266–272.

Arends, J. and Davidson, C.L. (1975) HPO_4^{2-} content in enamel and artificial carious lesions. Calcified Tissue Research 18, 65–79.

Ballon, J., Comparat V., and Pouxe J. (1983) The blade chamber: a solution for curved gaseous detector. Nuclear Instruments and Methods in Physics Research 217, 213–216.

Driessens, F.C.M. (1978) Physico-chemical interaction between biominerals and their environment. Berichte der Bunsen-Gesellschaft für Physikalische Chemie, 82, 312–320.

Elliott, J.C. (1964) The crystallographic structure of dental enamel and related apatites. PhD Thesis, University of London, London, U.K.

——(1994) Structure and chemistry of the apatites and other calcium orthophosphates, Elsevier, Amsterdam, The Netherlands.

——(1997) Structure, crystal chemistry and density of enamel apatites. In D.Chadwick and G. Cardew, Eds, Dental enamel, Ciba Foundation Symposium 205, p. 54–72, Wiley, Chichester, U.K.

Evain, M., Deniard, P., Jouanneaux, A., and Brec, R. (1993) Potential of the INEL X-ray position-sensitive detector: a general study of the Debye-Scherrer setting. Journal of Applied Crystallography, 26, 563–569.

Hayek, E. and Stadlemann, W. (1955) Darstellung von reinem Hydroxylapatit für Adsorptionszwecke. Angewandte Chemie, 67, 327.

Hendricks, S.B. and Hill, W.L. (1942) The inorganic constitution of bone. Science 96, 255–257.

Holcomb, D.W. and Young, R.A. (1980) Thermal decomposition of human tooth enamel. Calcified Tissue International, 31, 189–201.

Jeanjean, J., Vincent, U., and Fedoroff, M. (1994) Structural modification of calcium hydroxyapatite induced by sorption of cadmium ions. Journal of Solid State Chemistry, 108, 68–72.

Larson, A.C. and Von Dreele, R.B. (1986) GSAS, general structure analysis system. Los Alamos National Laboratory Report, LAUR 86–748.

Little, M.F. and Casciani, F.S. (1966) The nature of water in sound human enamel, a preliminary study. Archives of Oral Biology, 11, 565–571.

Michel, V., Ildefonse, P., and Morin, G. (1995) Chemical and structural changes in *Cervus elaphus* tooth enamels during fossilization (Lazaret Cave): a combined IR and XRD Rietveld analysis. Applied Geochemistry, 10, 145–159.

Nowotny, H. and Heger, G. (1986) Structure refinement of lead nitrate. Acta Crystallographica C42, 133–135.

Perdikatsis, B. (1991) X-ray powder diffraction study of francolite by the Rietveld method. Materials Science Forum, 79–82, 809–814.

Rodriguez-Lorenzo, L.M., Nicopoulos, S., Elliott, J.C., and Vallet-Regí, M., (1997) Rietveld and TEM studies of calcium deficient hydroxyapatite. Abstract PB4, Vol II, VIth European Conference on Solid State Chemistry, September 17–20, Eidgenössische Technische Hochschule, Zürich, Switzerland, Chairman R. Nesper.

Salinas, A.J., Serret, A., Vallet-Regí, M., and Hench L.L. (1997) Structure and solvation effects of PO_4^{3-}, HPO_4^{2-}, $H_2PO_4^-$ and H_3PO_4 from AM1 and PM3. In L. Sedel and C. Rey, Eds, Bioceramics Vol 10, Proceedings of the 10th International Symposium on Ceramics in Medicine, p. 245–248. Elsevier, Amsterdam, The Netherlands.

Sudarsanan, K. and Young, R.A. (1969) Significant precision in crystal structure details: Holly Springs hydroxyapatite. Acta Crystallographica B25, 1534–1543.

Trombe, J.-C. and Montel, G. (1971) Sur la préparation de l'oxyapatite phosphocalcique. Comptes Rendus des Séances de l'Académie des Sciences (Paris) Série C 273, 462–465.

Young, R.A. (1967) Dependence of apatite properties on crystal structural details. Transactions of the New York Academy of Sciences Series II 29, 949–959.

——(1993) The Rietveld method. Oxford University Press, U.K.

Young, R.A. and Mackie, P.E. (1980) Crystallography of human tooth enamel: initial structure refinement. Materials Research Bulletin, 15, 17–29.

MANUSCRIPT RECEIVED JULY 13, 1998
MANUSCRIPT ACCEPTED APRIL 20, 1999
PAPER HANDLED BY LEE A. GROAT